Surface Chemistry of SO_2 on Sn and Sn/Pt(111) Alloys: Effects of Metal−Metal Bonding on Reactivity toward Sulfur

José A. Rodriguez,* Tomas Jirsak, Sanjay Chaturvedi, and Jan Hrbek

Contribution from the Department of Chemistry, Brookhaven National Laboratory, Upton, New York 11973

Received June 22, 1998

Abstract: The surface chemistry of SO_2 on polycrystalline Sn, Pt(111), and a ($\sqrt{3}$ x $\sqrt{3}$)R30°-Sn/Pt(111) surface alloy has been investigated using synchrotron-based high-resolution photoemission and ab initio self-consistent field calculations. Metallic tin has a large chemical affinity for SO_2. At 100−150 K, SO_2 disproportionates on polycrystalline tin forming multilayers of SO_3 ($2SO_{2,a} \rightarrow SO_{gas} + SO_{3,a}$). At these low temperatures, the full dissociation of SO_2 ($SO_{2,a} \rightarrow S_a + 2O_a$) is minimal. As the temperature is raised to 300 K, the SO_3 decomposes, yielding SO_4, S, and O on the surface. Pure tin exhibits a much higher reactivity toward SO_2 than late transition metals (Ni, Pd, Pt, Cu, Ag, Au). In contrast, tin atoms in contact with Pt(111) interact weakly with SO_2. A ($\sqrt{3} \times \sqrt{3}$)R30°-Sn/Pt(111) alloy is much less reactive toward SO_2 than polycrystalline tin or clean Pt(111). At 100 K, SO_2 adsorbs molecularly on ($\sqrt{3} \times \sqrt{3}$)R30°-Sn/Pt(111). Most of the adsorbed SO_2 desorbs intact from the surface (250−300 K), whereas a small fraction dissociates into S and O. The drastic drop in reactivity when going from pure tin to the ($\sqrt{3} \times \sqrt{3}$)R30°-Sn/Pt(111) alloy can be attributed to a combination of ensemble and electronic effects. On the other hand, the low reactivity of the Pt sites in ($\sqrt{3} \times \sqrt{3}$)R30°-Sn/Pt(111) with respect to Pt(111) is a consequence of electronic effects. The Pt−Sn bond is complex, involving a Sn(5s,5p) → Pt(6s,6p) charge transfer and a Pt(5d) → Pt(6s,6p) rehybridization that localize electrons in the region between the metal centers. These phenomena reduce the electron donor ability of Pt and Sn, and both metals are not able to respond in an effective way to the presence of SO_2. The Sn/Pt system illustrates how a redistribution of electrons that occurs in bimetallic bonding can be useful for the design of catalysts that have a remarkably low reactivity toward SO_2 and for controlling sulfur poisoning.

I. Introduction

Platinum catalysts are widely used in oil refineries[1] and automobile exhaust system catalytic converters[2]. In general, these catalysts are very sensitive to sulfur poisoning.[1−3] Sulfur-containing molecules are common impurities in oil-derived feedstreams and fuels.[4] In automotive engines, these impurities react with oxygen to form SO_2 that decomposes on the Pt catalysts used in many exhaust system catalytic converters.[2a,5] S adatoms modify the electronic properties of Pt surfaces, inducing a large decrease in the density-of-states that the Pt 5d valence band has near the Fermi level.[6] This reduces the ability of Pt to respond to the presence of adsorbates,[6,7] and there is a drop in the chemical and catalytic activity of the metal. Thus, it is necessary to find ways to reduce the reactivity of Pt surfaces toward SO_2 and other sulfur-containing molecules. The use of mixed-metal systems may offer a route to accomplish this goal.[8] Bimetallic catalysts that contain Pt (X/Pt, X = Fe, Rh, Ni, Pd, Cu, Ag, Au, Zn, Sn) are frequently used in the oil and chemical industries,[1] and a major objective is to identify those systems that have a large catalytic activity and a high tolerance to the presence of sulfur-containing molecules in the feedstream or fuel.[2,3,8]

In principle, the formation of a metal−metal bond can induce a redistribution of electrons that affects the chemical properties of the bonded metals.[8−11] Platinum[12−17] and other group-10

* Corresponding author, FAX: 516-344-5815, E-mail: rodrigez@bnl.gov.

(1) (a) Somorjai, G. A. *Introduction to Surface Chemistry and Catalysis*; Wiley: New York, 1994. (b) Thomas, J. M.; Thomas, W. J. *Principles and Practice of Heterogeneous Catalysis*; VHC: New York, 1997. (c) Ertl, G.; Knözinger, H., Weitkamp, J., Eds. *Handbook of Heterogeneous Catalysis*; Wiley-VCH: New York, 1997.

(2) (a) Taylor, K. C. *Catal. Rev. Sci. Eng.* **1993**, *35*, 457. (b) Shelef, M.; Graham, G. W. *Catal. Rev. Sci, Eng.* **1994**, *36*, 433. (c) Rodriguez, J. A.; Goodman, D. W. *Surf. Sci. Rep.* **1991**, *14*, 1.

(3) (a) Bartholomew, C. H.; Agrawal, P. K.; Katzer, J. R. *Adv. Catal.* **1982**, *31*, 135. (b) Menon, P. G. *Chem. Rev.* **1994**, *94*, 1021. c. Oudar, J., Wise, H., Eds. *Deactivation and Poisoning of Catalysts*; Marcel Dekker: New York, 1986.

(4) Speight, J. G. *The Chemistry and Technology of Petroleum,* 2nd ed; Marcel Dekker: New York, 1991.

(5) Sun, Y.-M.; Sloan, D.; Alberas, D. J.; Kovar, M.; Sun, Z.-J.; White, J. M. *Surf. Sci.* **1994**, *319*, 34.

(6) (a) Rodriguez, J. A.; Kuhn, M.; Hrbek, J. *Chem. Phys. Lett.* **1996**, *251*, 13. (b) Rodriguez, J. A.; Chaturvedi, S.; Kuhn, M. *J. Chem. Phys.* **1998**, *108*, 3064.

(7) (a) Feibelman, P. J.; Hamann, D. R. *Surf. Sci.* **1985**, *149*, 48. (b) Feibelman, P. J. *Phys. Rev. B* **1991**, *43*, 9452.

(8) Rodriguez, J. A. *Surf. Sci. Rep.* **1996**, *24*, 223.

(9) (a) Wu, R. *Chem. Phys. Lett.* **1995**, *238*, 99. (b) Wu, R.; Freeman, A. J. *Phys. Rev. B* **1995**, *52*, 12419.

(10) Rodriguez, J. A.; Goodman, D. W. *Science*, **1992**, *257*, 897; *Acc. Chem. Res.* **1995**, *28*, 477.

(11) (a) Campbell, C. T. *Annu. Rev. Phys. Chem.* **1990**, *41*, 775. (b) Campbell, C. T. Bimetallic Model Catalysts. In ref 1c, Vol 2, pp 814−826.

(12) Rodriguez, J. A. *Surf. Sci.* **1996**, *345*, 347.

(13) Ross, P. *J. Vac. Sci. Technol. A* **1992**, *10*, 2546.

(14) Xu, C.; Koel, B. E. *Surf. Sci.* **1994**, *310*, 198.

(15) Paffett, M. T.; Gebhard, S. C.; Windham, R. G.; Koel, B. E. *J. Phys. Chem.* **1990**, *94*, *4*, 6831. Paffet, M. T.; Gebhard, S. C.; Windham, R. G.; Koel, B. E. *Surf. Sci.* **1989**, *223*, 449.

(16) Xu, C.; Koel, B. E. *Surf. Sci.* **1995**, *327*, 38.

10.1021/ja982174a CCC: $15.00
Published on Web 10/16/1998

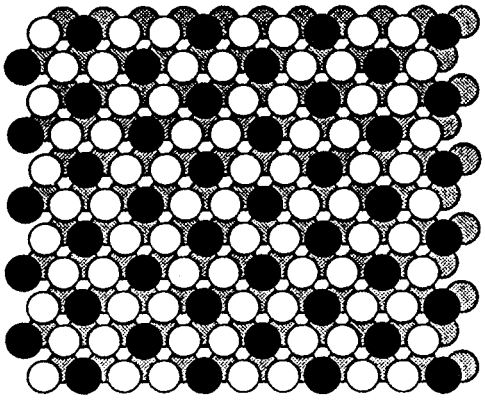

Figure 1. Structure of the ($\sqrt{3} \times \sqrt{3}$)R30°-Sn/Pt(111) surface alloy (from ref 23). The dark circles represent Sn atoms, while the open and shaded circles denote first and second layer Pt atoms, respectively.

metals[8,10,17] are very sensitive to the effects of metal−metal bonding. In the S_2/Ag/Pt(111)[18] and S_2/Cu/Pt(111)[19] systems, Ag and Cu *promote* Pt ↔ S interactions and the formation of platinum sulfides. This is clearly a type of situation that one wants to avoid. In a previous work,[20] we found that Sn/Pt alloys are reactive toward H_2S and S_2 less than the individual metals (pure Pt and Sn). It is worthwhile to test if the same trend is valid for SO_2. A priori, however, this assumption may not hold because tin forms very stable compounds with sulfur oxides.[21] Thus, the Sn adatoms could enhance the reactivity of a Pt surface toward SO_2 instead of reducing it.

Well-defined alloys of Pt−Sn can be prepared by depositing Sn on Pt(111) and annealing the Sn/Pt(111) system at elevated temperatures.[22−24] This produces ordered surface alloys in which the Sn surface atoms are located approximately in the plane of the substrate surface (as opposed to an ordered metal overlayer).[22−24] Figure 1 shows the structural geometry of a ($\sqrt{3} \times \sqrt{3}$)R30°-Sn/Pt(111) surface alloy.[23] Sn atoms are present only in the top layer and protrude 0.22 Å out of the plane of Pt atoms.[23,24] Each Pt atom present in the surface has the same number of Pt and Sn neighbors (3 and 3). In the alloy, there are plenty of a-top and bridge Pt sites that can adsorb and dissociate small molecules such as S_2, H_2S, and SO_2. The chemical properties of the ($\sqrt{3} \times \sqrt{3}$)R30°-Sn/Pt(111) surface alloy has been examined in detail.[13−16,25] Depending on the type of adsorbate, Sn can modify the reactivity of the Pt(111) substrate through structural or electronic effects.[8,11]

In this work, we examine the surface chemistry of SO_2 on polycrystalline Sn, Pt(111) and a ($\sqrt{3} \times \sqrt{3}$)R30°-Sn/Pt(111) surface alloy using synchrotron-based high-resolution photoemission an ab initio self-consistent field (SCF) calculations. The adsorption of SO_2 on Pt(111) has been the subject of several studies.[5,26,27] At 100 K, SO_2 adsorbs molecularly on Pt(111), whereas at 300 K the molecule dissociates and forms SO_3/SO_4 species on the metal surface. We observe a different behavior for SO_2 on ($\sqrt{3} \times \sqrt{3}$)R30°-Sn/Pt(111). Alloying induces drastic changes in the reactivity of the bonded metals. The Sn/Pt system illustrates how electronic perturbations that occur in bimetallic bonding can be useful for the design of catalysts that have a low reactivity toward SO_2 and other sulfur-containing molecules.

II. Experimental and Theoretical Methods

II.1. Instrumentation and Sample Preparation. The photoemission experiments were performed at the U7A beamline of the National Synchrotron Light Source (NSLS) in an ultrahigh-vacuum chamber (base pressure ~6×10^{-10} Torr) that was equipped with a hemispherical electron-energy analyzer and a Mg Kα X-ray source for X-ray photoelectron spectroscopy (XPS). The S 2p and Pt 4f spectra were acquired using the beam from the synchrotron at a photon energy of 260 eV. The binding energy of these spectra was calibrated by the position of the Fermi edge. Unmonochromatized Mg Kα radiation was used to acquire the Sn 3d and O 1s spectra. In these XPS spectra, the binding energy was calibrated by setting the $3d_{5/2}$ level of a thick Sn multilayer at 484.9 eV.[28]

The Pt(111) crystal was cleaned by following procedures reported in the literature.[20,22,23] Sn, S, and O were removed from the surface by sputtering and annealing cycles. The Pt(111) sample was spot-welded to a manipulator capable of resistive heating to 1200 K and liquid nitrogen cooling to 80 K. Heating to 1800 K could be achieved by electron bombardment from behind the sample. A W-5%Re/W-26%Re thermocouple was attached to the edge of the sample for temperature measurements.

Tin was vapor-deposited by heating an ultrapure ingot of the metal. The Sn ingot was placed in a Ta crucible which was heated resistively.[20] The ($\sqrt{3} \times \sqrt{3}$)R30°-Sn/Pt(111) surfaces were prepared using the methodology described in ref 23. The formation of the Pt−Sn alloys was verified using low-energy electron diffraction (LEED).[22,23] Polycrystalline surfaces of tin were generated by depositing very thick multilayers of the metal on the Pt(111) substrate at 100 K with subsequent annealing to 300 K. In these systems, there was a complete disappearance of the Pt XPS peaks. Polycrystalline Sn, Pt(111), and the ($\sqrt{3} \times \sqrt{3}$)R30°-Sn/Pt(111) alloy were exposed to SO_2 (high purity from Mattheson) at 100 and 300 K. The purity of the SO_2 gas was confirmed using a mass spectrometer. The coverage of sulfur (or oxygen) on the surface was determined by measuring the area under the S 2p (or O 1s) spectra which was scaled to absolute units by comparing to the corresponding area for 0.33 ML of S on Pt(111)[6,18] (or 0.25 ML of O on Pt(111)[29]). In this work, coverages are reported with respect to the number of Pt(111) surface atoms (1.51×10^{15} atoms/cm^2). One O or S adatom per substrate surface atom corresponds to $\theta = 1$ monolayer (ML).

II.2. Molecular Orbital Calculations. We investigated the bonding interactions of SO_2 with Pt(111) and ($\sqrt{3} \times \sqrt{3}$)R30°-Sn/Pt(111) using cluster models (Pt_{12}, Pt_{15}, Sn_3Pt_9, Sn_4Pt_{11}). The ab initio SCF calculations described in section III.3. were carried out using the HONDO program.[30] Since the systems under consideration have a large number of heavy atoms, sulfur and oxygen were the only elements for

(17) Hammer, B.; Morikawa, Y.; Nørskov, J. K. *Phys. Rev. Lett.* **1996**, *76*, 2141.
(18) (a) Kuhn, M.; Rodriguez, J. A. *J. Catal.* **1995**, *154*, 355. (b) Rodriguez, J. A.; Kuhn, M.; Hrbek, J. *J. Phys. Chem.* **1996**, *100*, 15494.
(19) Kuhn, M.; Rodriguez, J. A. *Catal. Lett.* **1995**, 32, 345.
(20) Rodriguez, J. A.; Chaturvedi, S.; Jirsak, T.; Hrbek, J. *J. Chem. Phys.* **1998**, 109, 4052.
(21) Dean, J. A., Ed. *Lange's Handbook of Chemistry*, 13th ed; McGraw-Hill: New York, 1985; Table 9-1.
(22) Paffett, M. T.; Windham, R. G. *Surf. Sci.* **1989**, *208*, 34.
(23) Overbury, S. H.; Mullins, D. R.; Paffett, M. T.; Koel, B. E. *Surf. Sci.* **1991**, *254*, 45.
(24) Overbury, S. H.; Ku, Y.-S. *Phys. Rev. B* **1992**, *46*, 7868.
(25) (a) Xu, C.; Peck, J. W.; Koel, B. E. *J. Am. Chem. Soc.* **1993**, *115*, 751. (b) Szanyi, J.; Paffett, M. T. *J. Am. Chem. Soc.* **1995**, *117*, 1034. (c) Heitzinger, J. M.; Gebhard, S. C.; Koel, B. E. *J. Phys. Chem.* **1993**, *97*, 5327. (d) Xu, C.; Koel, B. E.; Paffett, M. T. *Langmuir* **1994**, *10*, 166.
(26) Polcik, M.; Wilde, L.; Haase, J.; Brena, B.; Comelli, G.; Paolucci, G. *Surf. Sci.* **1997**, *381*, L568.
(27) (a) Wilson, K.; Hardacre, C.; Baddeley, C. J.; Lüdecke, J.; Woodruff, D. P.; Lambert, R. M. *Surf. Sci.* **1997**, *372*, 279. (b) Astegger, S.; Bechtold, E. *Surf. Sci.* **1982**, *122*, 491. (c) Köhler, U.; Wassmuth, H.-W. *Surf. Sci.* **1983**, *126*, 448.
(28) Williams, G. P. *Electron Binding Energies of the Elements, Version II*; National Synchrotron Light Source, Brookhaven National Laboratory, 1992.
(29) Puglia, C.; Nilsson, A.; Herrnås, B.; Karis, O.; Bennich, P.; Mårtensson, N. *Surf. Sci.* **1995**, *342*, 119.
(30) Dupuis, M.; Chin, S.; Marquez, A. In *Relativistic and Electron Correlation Effects in Molecules and Clusters*; Malli, G. L., Ed.; NATO ASI Series; Plenum: New York, 1992.

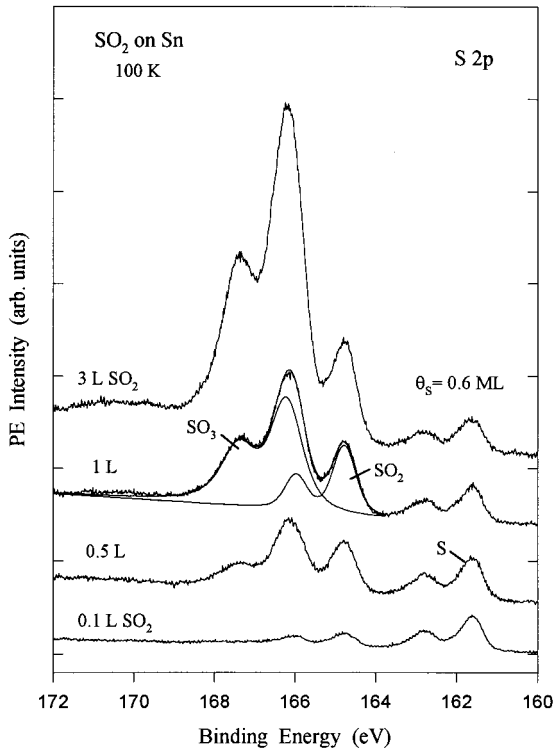

Figure 2. S 2p spectra for the adsorption of SO_2 on polycrystalline tin at 100 K. All of the spectra were acquired using a photon energy of 260 eV. The spectrum for a SO_2 dose of 1 L was curve-fitted following the procedure described in ref 6.

which we included all of their electrons in the ab initio calculations. The atomic orbitals of sulfur and oxygen were expressed in terms of double-ζ quality basis sets augmented with polarization functions.[20,30,31] Sn and Pt were described using the effective-core potentials and basis sets employed in our previous study for the adsorption of H_2S and S_2 on $(\sqrt{3} \times \sqrt{3})$R30°-Sn/Pt(111).[20] For these elements, we treated explicitly only the valence shells: 5s and 5p orbitals of Sn,[20,32] plus 5d and 6s,p orbitals of Pt.[20,33] Previous experience indicates that these basis sets provide satisfactory results for the adsorption geometries of sulfur-containing molecules.[6,20] On the other hand, the energetics derived from these SCF calculations for adsorption reactions are not quantitative and simply provide a guide for the interpretation of experimental results.[6,20,33] The size of the basis sets, the use of finite clusters, and the lack of electron correlation introduce uncertainty in the computed bonding energies.[34,35] Despite this limitation, the use of ab initio SCF methods with cluster models has proved to be a very useful approach for studying a large variety of surface phenomena.[34,35]

III. Results and Discussion

III.1. Reaction of SO_2 with Polycrystalline Tin. Figure 2 shows S 2p spectra acquired after dosing SO_2 to polycrystalline tin at 100 K. A dose of 0.1 L of SO_2 produces a spectrum that has two doublets with the $2p_{3/2}$ components at 161.6 and 164.7 eV. The peak at 161.6 eV matches well the S $2p_{3/2}$ binding energies seen for atomic S on tin.[20] The peak at 164.7 eV can be assigned to molecularly chemisorbed SO_2.[5,26] Thus, for very small exposures of SO_2 at 100 K, one has molecular and dissociative ($SO_{2,gas} \rightarrow S_a + 2O_a$) adsorption of SO_2. Now, the amount of SO_2 that dissociates is very small ($\theta_S \approx 0.05$ ML), and the S 2p features for atomic sulfur do not grow when the doses of SO_2 are increased. It is likely that SO_2 is fully dissociating on a few tin sites of the polycrystalline surface that are very reactive. Once these sites are saturated with S and O, one sees another type of chemistry when the coverage of SO_2 is substantial. After a SO_2 dose of 0.5 L, new S 2p features appear between 166 and 168 eV. These new features appear at the position reported for SO_3 species,[36] and at a binding energy significantly lower than that expected for SO_4 species.[36,37] Thus, we assign them to adsorbed SO_3. The small peaks seen for atomic sulfur rule out the formation of SO_3 through the following process:

$$SO_{2,gas} \rightarrow S_a + 2O_a \quad (1)$$

$$SO_{2,gas} + O_a \rightarrow SO_{3,a} \quad (2)$$

The SO_3 is probably being formed through a disproportionation reaction

$$2SO_{2,a} \rightarrow SO_{3,a} + SO_{gas} \quad (3)$$

The small S 2p peaks for atomic sulfur also rule out a disproportionation of the type

$$2SO_{2,a} \rightarrow SO_{4,a} + S_a \quad (4)$$

In Figure 2, a SO_2 dose of 3 L produces a total sulfur coverage of 0.6 ML and the dominant species on the surface is SO_3. At this point, the high sulfur and oxygen coverages indicate the penetration of the adsorbate into the subsurface region. The S 2p features for SO_3 kept growing after raising the doses of SO_2 with sulfur coverages that were well above 1 ML.

The top spectrum in Figure 3 was taken after a large dose (15 L) of SO_2 to tin at 100 K. The spectrum is well fitted by a set of two doublets that correspond to physisorbed SO_2 and a Sn_xSO_3 film. Upon heating the sample to 150 K, the peaks for the SO_2 multilayer disappear, and the S 2p spectrum is dominated by the SO_3 features with a very small trace for atomic sulfur around 162 eV. Further heating to 300 K induces the decomposition of Sn_xSO_3 and drastic changes in the S 2p region. S appears (probably SnS_z)[20] and a new feature is seen at ~167 eV that can be attributed to SO_4 formed through the reaction

$$Sn_xSO_3 \rightarrow Sn_ySO_4 + SnS_z + SnO_m \quad (5)$$

The last S 2p spectrum is similar to spectra obtained after exposing polycrystalline tin to SO_2 at 300 K (not shown).

The O 1s and Sn 3d XPS results displayed in Figures 4 and 5 support the "picture" derived from the analysis of the S 2p data. Upon a dose of 0.1 L, the O 1s region (Figure 4) exhibits weak features that can be assigned to a mixture of O and SO_2.[5,26] Additional doses of SO_2 produce O 1s features centered at 531.4−531.7 eV that cannot be attributed to SO_2[5,36] or SO_4[36]

(31) Chaturvedi, S.; Rodriguez, J. A.; Hrbek, J. *Surf. Sci.* **1997**, *384*, 260.

(32) Wadt, W. R.; Hay, P. J. *J. Chem. Phys.* **1985**, *82*, 284.

(33) (a) Rodriguez, J. A.; Kuhn, M. *J. Phys. Chem.* **1994**, *98*, 11251. (b) Rodriguez, J. A.; Kuhn, M. *J. Chem. Phys.* **1995**, *102*, 4279. (c) Rodriguez, J. A. *Surf. Sci.* **1996**, *345*, 347. (d) Rodriguez, J. A.; Kuhn, M. *Chem. Phys. Lett.* **1995**, *240*, 435. (e) Zhang, L.; Kuhn, M.; Diebold, U.; Rodriguez, J. A. *J. Phys. Chem. B* **1997**, *101*, 4588.

(34) (a) Whitten, J. L.; Yang, H. *Surf. Sci. Rep.* **1996**, *24*, 55. (b) van Santen, R. A.; Neurock, M. *Catal. Rev. Sci.-Eng.* **1995**, *37*, 557.

(35) Ruette, F., Ed. *Quantum Chemistry Approaches to Chemisorption and Catalysis*; Kluwer: Dordrecht, 1992.

(36) Wagner, C. D., Riggs, W. M., Davis, L. E., Moulder, J. F., Muilenberg, G. E., Eds. *Handbook of X-ray Photoelectron Spectroscopy*; Perkin-Elmer: Eden Prairie, MN, 1978; pp 42, 56, and 118.

(37) (a) In ref 37b, a difference of 5−5.5 eV is observed between the S 2p binding energies of S and SO_4 on alumina. A separation of ~5 eV is reported in ref 26 for the S $2p_{3/2}$ binding energies of S and SO_4 on Pt(111), whereas a difference of ~3 eV is observed between the S $2p_{3/2}$ binding energies of chemisorbed S and SO_2. (b) Wilson, K.; Lee, A. F.; Hardacre, C.; Lambert, R. M. *J. Phys. Chem. B* **1998**, *102*, 1736.

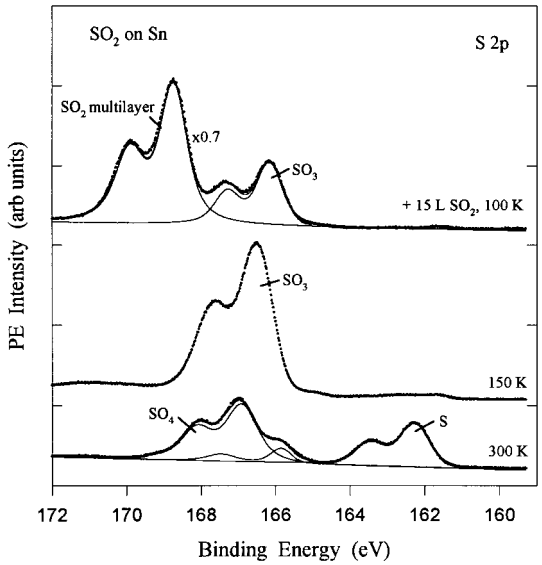

Figure 3. S 2p spectra recorded after dosing 15 L of SO_2 to polycrystalline tin at 100 K, with subsequent annealing to 150 and 300 K. The electrons were excited using a photon energy of 260 eV. The spectrum at the top was curve-fitted following the procedure described in ref 6.

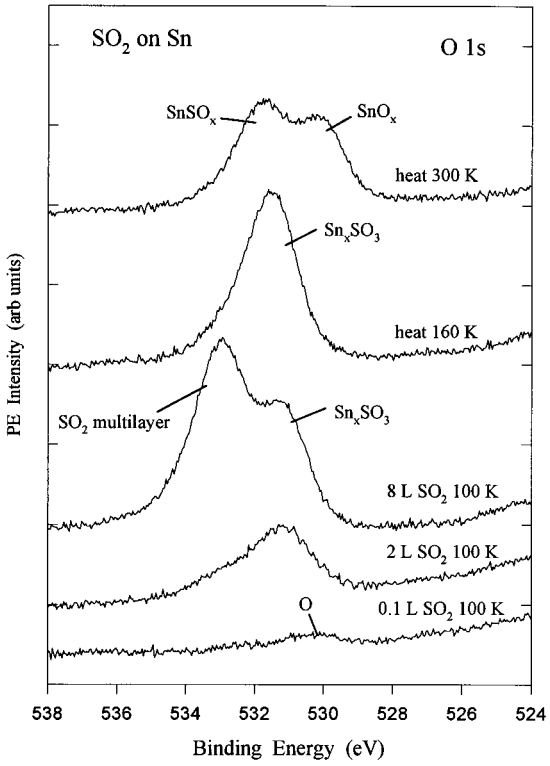

Figure 4. O 1s XPS spectra for the adsorption of SO_2 on polycrystalline tin. The surface was exposed 0.1, 2, and 8 L of SO_2 at 100 K. This was followed by annealing to 160 and 300 K. The spectra were acquired using Mg Kα radiation.

but match well the O 1s peak position reported for SO_3.[36] In the O 1s spectra for the SO_2 doses of 2 and 8 L, there is no significant signal in the region where atomic oxygen appears ($\sim$ 530 eV), which is consistent with the formation of SO_3 according to reaction 3. The features for Sn_xSO_3 dominate the O 1s region after heating the sample from 100 to 160 K. At this point, the corresponding Sn 3d spectrum (Figure 5) indicates the existence of two types of tin species, pure metallic Sn and Sn bonded to SO_3, that exhibit a separation of $\sim$1.7 eV in their

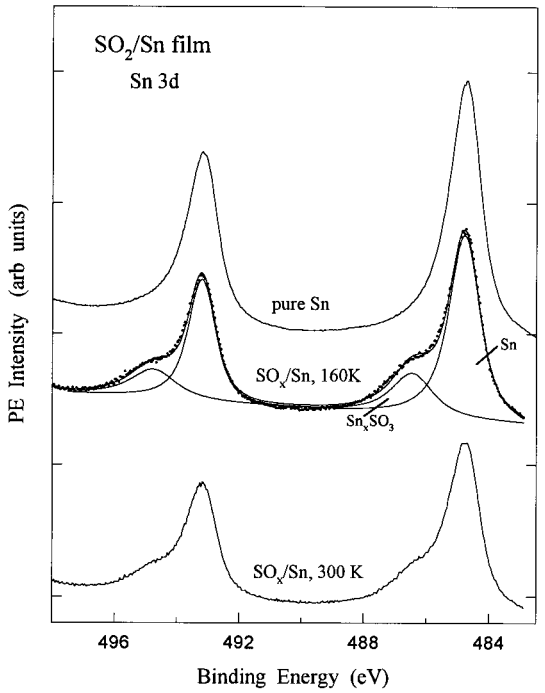

Figure 5. Sn 3d XPS spectra for pure metallic tin and a polycrystalline surface of the metal exposed to a multilayer of SO_2 at 100 K and subsequently heated to 160 and 300 K. The two spectra at the bottom were acquired in the same set of experiments that produced the O 1s spectra in Figure 4. The electrons were excited using Mg Kα radiation.

binding energies. A similar separation is found when comparing the Sn 3d binding energies of Sn and SnO or SnS.[36] After the sample is annealed to 300 K, the O 1s and Sn 3d spectra point toward the presence of $SnSO_x$ and SnO_x. These data together with the S 2p data in Figure 3 suggest that at temperatures between 200 and 300 K Sn_xSO_3 decomposes via reaction 5.

In a set of experiments, we investigated the adsorption of SO_2 on polycrystalline tin at 300 K. Again we observed a very large reactivity. At SO_2 doses below 0.5 L, there was extensive dissociation of the molecule that produced substantial coverages of S and O on the surface. For SO_2 doses above 0.5 L, SO_3 and SO_4 were formed on the surface. As the doses of SO_2 were increased, the S 2p peaks for atomic S and the SO_3/SO_4 species grew simultaneously. The typical S 2p spectra exhibited a lineshape similar to that of the spectrum at the bottom of Figure 3. Under these conditions, adsorbed SO_3 and SO_4 were likely formed by the reaction of SO_2 with surface O because the probability for $SO_{2,a} \leftrightarrow O_a$ interactions was much larger than the probability for $SO_{2,a} \leftrightarrow SO_{2,a}$ interactions and a disproportionation reaction. At 300 K, the sticking coefficient of SO_2 on polycrystalline tin was smaller than at 100 K, but at room temperature we were still able to form multilayers of $SnSO_x$, SnO_m, and SnS_z with SO_2 doses of 5−10 L.

When compared to late transition metals (Ni, Pd, Pt, Cu, Ag and Au),[5,26,27,38] tin shows an extremely high reactivity toward SO_2. The late transition metals only chemisorb SO_2 molecularly at 100 K (i.e., no formation of SO_3 or SO_4). On these metals, the reaction with SO_2 at 300 K produces saturation coverages of S, O, and SO_x species that are at the submonolayer level.[5,26,27,38] This is not the case on tin, where total sulfur coverages well above a monolayer are relatively easy to produce, and the sulfur species penetrate into the bulk of the sample. SO_2 virtually corrodes metallic tin under UHV conditions. This

(38) Haase, J. *J. Phys: Condens. Matter* **1997**, *9*, 3647 and references therein.

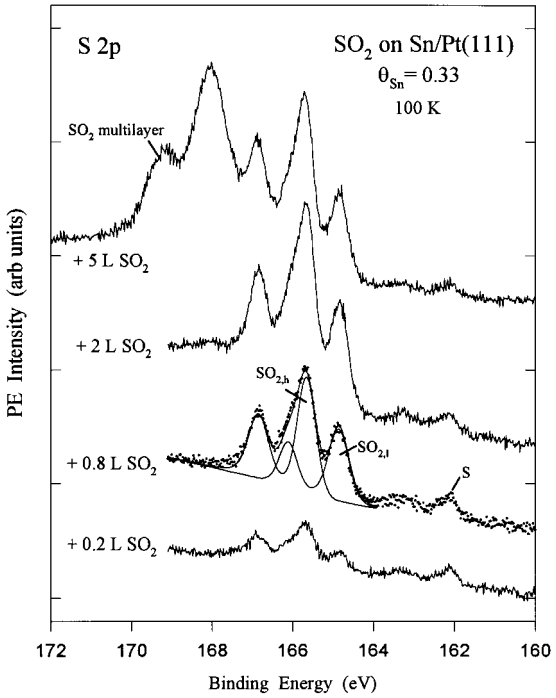

Figure 6. S 2p spectra for the adsorption of SO_2 on a $(\sqrt{3} \times \sqrt{3})$R30°-Sn/Pt(111) surface alloy at 100 K. The spectra were taken using a photon energy of 260 eV.

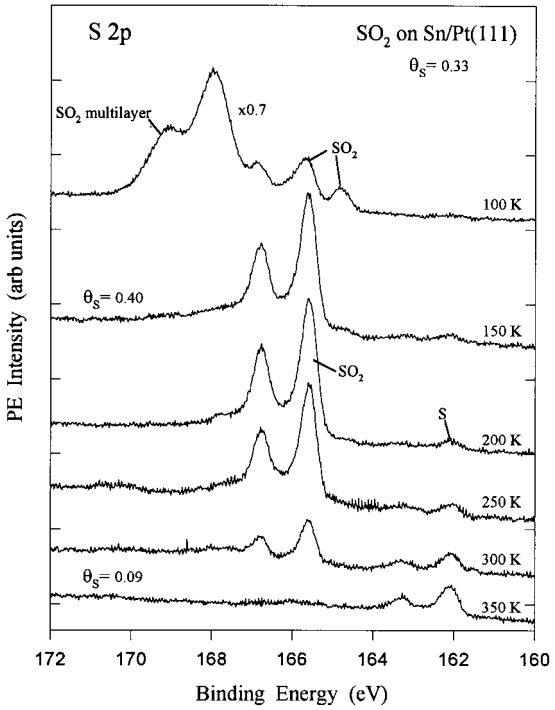

Figure 7. S 2p spectra acquired after saturating a $(\sqrt{3} \times \sqrt{3})$-R30°-Sn/Pt(111) surface alloy with SO_2 at 100 K and subsequent annealing to 150, 200, 250, 300, and 350 K. The electrons were excited using a photon energy of 260 eV.

phenomenon is made possible by the large thermochemical stability of tin sulfites and sulfates.[21]

III.2. Reaction of SO_2 with Pt(111) and $(\sqrt{3} \times \sqrt{3})$-R30°-Sn/Pt(111). The chemistry of SO_2 on Pt(111) has been examined in detail using several techniques for surface characterization.[5,26,27] At 100 K, SO_2 adsorbs molecularly on Pt(111). Two different adsorption states can be detected in photoemission,[26] and in one of them SO_2 is probably bonded in a η^2-S,O conformation with its molecular plane nearly perpendicular to the surface.[5,26,27a] The chemisorbed SO_2 dissociates or reacts at temperatures above 250 K, forming a mixture of S, O, and SO_4 on the surface. A similar mixture is obtained after dosing SO_2 to Pt(111) at 300 K. The adsorbed SO_4 species are stable up to temperatures well above 400 K.[26,27]

Figure 6 shows S 2p spectra acquired after dosing SO_2 to a $(\sqrt{3} \times \sqrt{3})$R30°-Sn/Pt(111) surface alloy at 100 K. A small signal (~0.03 ML) is seen for atomic sulfur around 162.2 eV, but most of the adsorbed SO_2 is intact on the surface. A SO_2 dose of 0.8 L produces two clear molecular adsorption states. After examining their peak positions and binding-energy separations with respect to atomic S (3.4−2.6 eV), we can conclude that they correspond to chemisorbed SO_2.[26,37] The S 2p binding energies of these states are not high enough to assign them to SO_3 or SO_4.[36,37] Similar states are observed on Pt(111),[26] but not on polycrystalline tin where the dominant species is SO_3 (see Figures 2 and 3).

Figures 7 and 8 display photoemission spectra (S 2p, O 1s, Sn 3d) recorded after saturating a $(\sqrt{3} \times \sqrt{3})$R30°-Sn/Pt(111) alloy with SO_2 at 100 K and sequential heating to 350 K. At 100 K, one has physisorbed and chemisorbed SO_2 on the surface. By 150 K, the SO_2 multilayer has desorbed, and essentially there is only one type of S species on the surface (see Figure 7 and notice the well-defined doublet). The ratio of the oxygen and sulfur coverages ($\theta_O/\theta_S = 0.76/0.40$) is close to two as expected for SO_2. At the same time, the S 2p and O 1s peak positions are near those reported for chemisorbed SO_2 on Pt(111)[26,37] and much too low to be attributed to SO_3 or SO_4.[36,37] The corresponding Sn 3d spectrum (bottom panel in Figure 8) shows shifts of ~0.4 eV with respect to the peak positions for the clean $(\sqrt{3} \times \sqrt{3})$R30°-Sn/Pt(111) alloy. These shifts are much smaller than those seen in Figure 5 (~1.7 eV) for the SO_2/Sn system, indicating that the interactions between SO_2 and the admetal are weak in the $(\sqrt{3} \times \sqrt{3})$R30°-Sn/Pt(111) alloy. From 150 to 200 K, there are no significant changes in the S 2p region (Figure 7). A minor decrease in the SO_2 signal and an increase in the S signal are observed upon annealing to 250 K. Substantial changes occur when heating from 250 to 300 K; 0.23 ML of SO_2 dissappear from the surface (~ 65% of the SO_2 coverage at 250 K) while 0.02 ML of S are formed. Most of the SO_2 desorbs into the gas phase, and no adsorbed SO_3 or SO_4 is formed. A final annealing to 350 K leads to the complete disappearance of SO_2, leaving small coverages of atomic S (0.09 ML) and O (0.16 ML) on the surface. At this point, the Sn 3d spectrum (bottom of Figure 8) shows broad peaks that contain contributions from two tin species. Eighty-two percent of the tin adatoms exhibit Sn 3d binding energies that are close to those of $(\sqrt{3} \times \sqrt{3})$R30°-Sn/Pt(111), whereas the remaining 18% display binding-energy shifts of ~ 0.9 eV. Although large, these binding-energy shifts are still smaller than those seen for SnO_x and SnS_x.[20,36]

In the case of SO_2/Pt(111),[5,26] experiments similar to those in Figures 7 and 8 produce a larger amount of atomic S (40−50% of the SO_2 adsorbed at 150 K dissociates into S) and SO_4 species that decompose at temperatures above 400 K. Thus, the $(\sqrt{3} \times \sqrt{3})$R30°-Sn/Pt(111) alloy is less reactive toward SO_2 than either polycrystalline tin or Pt(111). This behavior is very clear in Figure 9, where we compare the total amount of sulfur (SO_4, SO_3, SO_2, and S) adsorbed after dosing SO_2 to these three systems at 300−310 K. Pure tin is much more reactive than Pt(111). This can be expected since the tin surface has a larger roughness than Pt(111), and tin also has a higher

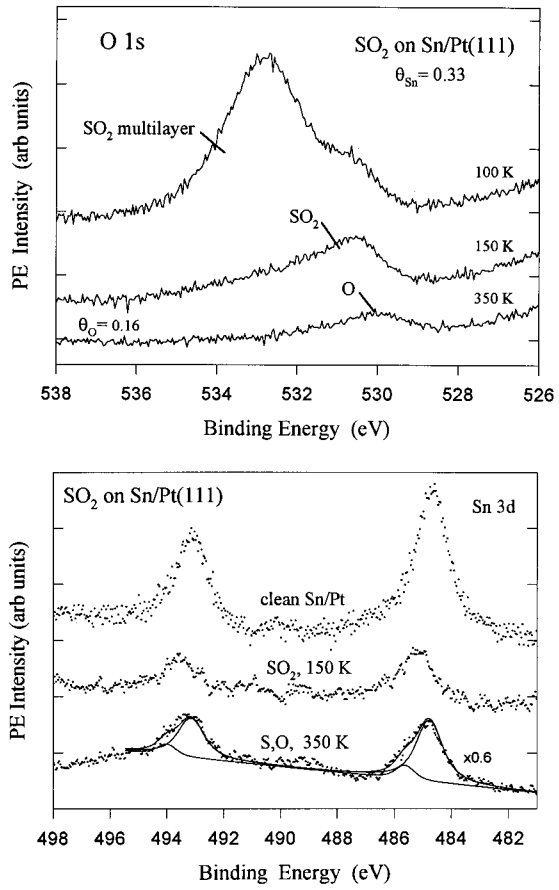

Figure 8. O 1s and Sn 3d XPS spectra taken after depositing a multilayer of SO_2 on $(\sqrt{3} \times \sqrt{3})$R30°-Sn/Pt(111) at 100 K, followed by annealing to 150 and 350 K. The spectra were acquired using Mg Kα radiation. These data were obtained during the experiments that produced the S 2p spectra in Figure 7.

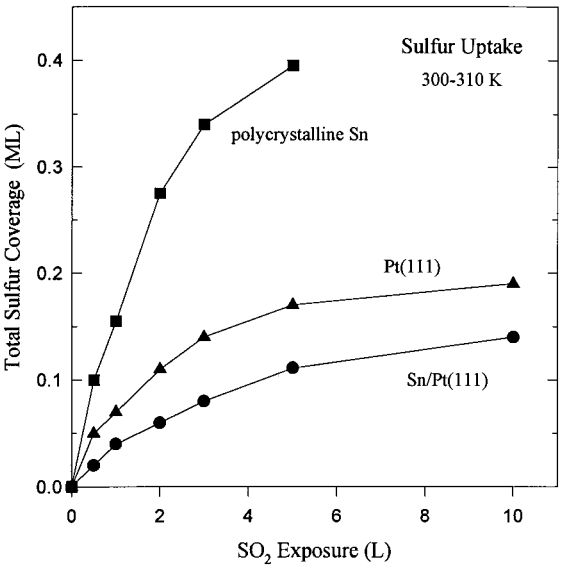

Figure 9. Total amount of sulfur ($SO_4 + SO_3 + SO_2 + S$) deposited on polycrystalline Sn, Pt(111), and a $(\sqrt{3} \times \sqrt{3})$R30°-Sn/Pt(111) surface alloy after several doses of SO_2 at 300−310 K. The coverage of sulfur was determined by measuring the area under the S 2p features (see Section II.1).

chemical affinity for S, O, and SO_x species than Pt (for example, compare the heats of formation for the corresponding bulk compounds in ref 21). In principle, one could expect that Sn adatoms would enhance the ability of the Pt(111) surface to adsorb and dissociate SO_2. However, the $(\sqrt{3} \times \sqrt{3})$-R30°-Sn/Pt(111) alloy exhibits a reactivity smaller than that of pure Sn or Pt(111). Under the conditions of Figure 9, the amount of O on the surface alloy was not large (<0.25 ML), and the $SO_2 \leftrightarrow$ O interactions were less important than the $SO_2 \leftrightarrow$ metal interactions. This can change at large coverages of O (>0.35 ML). One can induce the reaction of O_2 with $(\sqrt{3} \times \sqrt{3})$R30°-Sn/Pt(111) to form SnO_x/Pt(111).[39] We have found that the rate of adsorption of SO_2 on SnO_x/Pt(111) is somewhat larger than on Pt(111) or $(\sqrt{3} \times \sqrt{3})$R30°-Sn/Pt(111). But in this case, one has a different type of system, and the SO_2 mostly interacts with the oxygen sites of the SnO_x/Pt(111) surface to yield adsorbed SO_3 and SO_4 species.

The trends in Figure 9 are very similar to those found after dosing S_2 and H_2S to polycrystalline Sn, Pt(111), and $(\sqrt{3} \times \sqrt{3})$R30°-Sn/Pt(111).[20] Thus, it appears that the surface alloy in general has a remarkably low reactivity toward sulfur-containing molecules independently of the type of atom to which sulfur is bonded.[40] Bimetallic bonding substantially reduces the reactivity of Sn and also has a negative effect on the reactivity of Pt. When comparing polycrystalline Sn and $(\sqrt{3} \times \sqrt{3})$-R30°-Sn/Pt(111), it may be argued that the lower reactivity of the alloy is due to the fact that this system does not have adsorption sites with two or three adjacent tin atoms (see Figure 1). It is not expected that a single tin atom will be able to accomplish the type of surface chemistry seen in Figures 2 and 3 for SO_2/Sn. Therefore, the drop in the reactivity observed when going from metallic Sn to $(\sqrt{3} \times \sqrt{3})$R30°-Sn/Pt(111) can be attributed to "ensemble effects" (i.e., a simple partition of the active sites formed by a group of adjacent tin atoms).[11] However, the differences in reactivity between Pt(111) and $(\sqrt{3} \times \sqrt{3})$R30°-Sn/Pt(111) can only be explained invoking "electronic effects".[11] In the $(\sqrt{3} \times \sqrt{3})$R30°-Sn/Pt(111) surface alloy, there are plenty of adsorption sites with two or three adjacent Pt atoms (see Figure 1), and some Pt atoms are being replaced with Sn atoms that, in principle, should be more reactive. Thus, the low reactivity of the alloy must be a consequence of the electronic perturbations induced by the formation of Pt−Sn bonds. In the next section, we will examine these electronic effects at a molecular orbital level using ab initio SCF calculations and cluster models.

III.3. Bonding of SO_2 to Pt(111) and $(\sqrt{3} \times \sqrt{3})$-R30°-Sn/Pt(111). Figure 10 shows the metal clusters employed to model the Pt(111) and $(\sqrt{3} \times \sqrt{3})$R30°-Sn/Pt(111) surfaces. Cluster II (Sn_4Pt_{11}) represents a "cut" in the structure shown in Figure 1 for the $(\sqrt{3} \times \sqrt{3})$R30°-Sn/Pt(111) alloy. In these clusters, we used the geometry reported for bulk Pt[41] and the Sn/Pt alloy.[42] Previous studies have shown that clusters of this

(39) (a) Logan, A. D.; Paffett, M. T. *J. Catal.* **1992**, *133*, 179. (b) To be published. It is much easier to form SnO_x/Pt(111) than SnS_x/Pt(111) because the heats of formation of tin oxides are 50−100 kcal/mol more exothermic than those of tin sulfides.[21]

(40) (a) This has been proved to be valid for sulfur bonded to S, H, and O. The reactivity seen for H_2S is expected to be representative of the reactivity of thiols (RSH).[40b] The test with SO_2 is more demanding than those with H_2S or S_2, because from a thermochemical viewpoint,[21] tin sulfates ($SnSO_x$) are much more stable than tin sulfides (SnS_x). (b) Rodriguez, J. A. *Surf. Sci.* **1990**, *234*, 421; **1992**, *278*, 326.

(41) Kittel, C. *Introduction to Solid State Physics*, 6th ed; Wiley: New York, 1986; pp 23 and 24.

(42) We replaced four Pt atoms in the first layer of cluster I with four Sn atoms. Following the results of low-energy alkali ion scattering,[24] the Sn atoms were located 0.22 Å above the plane of the first layer Pt atoms. This produced a Sn−Pt nearest-neighbor distance of 2.78 Å, which is somewhat shorter than the corresponding distance found in a bulk Pt_3Sn alloy (2.83 Å).[24]

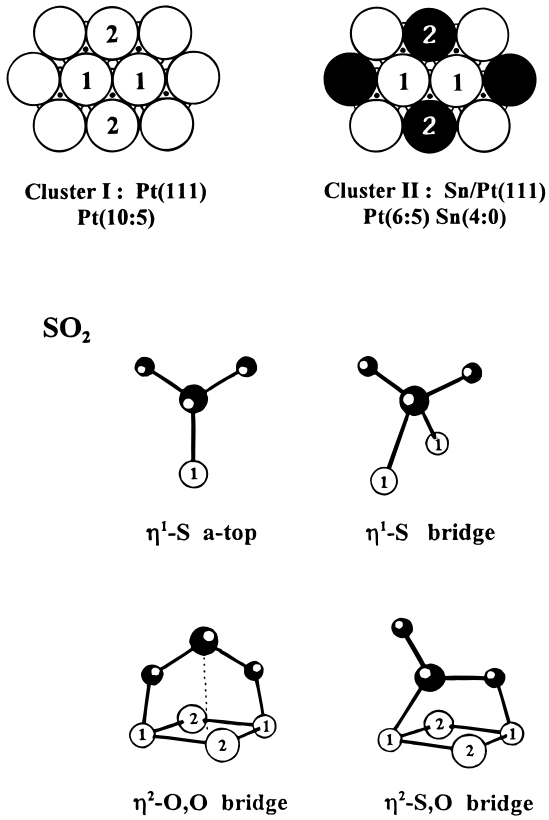

Figure 10. In the top of the figure are shown the clusters used to model the Pt(111) and ($\sqrt{3} \times \sqrt{3}$)R30°-Sn/Pt(111) surfaces. Each cluster has 15 metal atoms arranged in two layers. The notation (a:b) indicates how many metal atoms are in each layer. The (•) indicate hollow sites that have a Pt atom underneath in the second layer. The Pt atoms that form the adsorption sites are labeled "1". The bottom part of the figure shows the bonding configurations for SO_2. In all of these configurations, the molecule was adsorbed with its molecular plane perpendicular to the surface.

Table 1. Pt_n and Pt_mSn_l Clusters: Atomic Orbital Populations and Charges (Electrons)

	Pt orbital populations				
	5d	6s	6p	Pt atom charge	Sn atom charge
Pt_{15}[a]	9.34	0.61	0.09	−0.04	
$Pt_{11}Sn_4$[a,b]	9.11	0.82	0.23	−0.16	+0.23
Pt_8[c]	9.37	0.51	0.12	0.00	
Pt_4Sn_4[c]	9.08	0.89	0.17	−0.14	+0.14

[a] The values listed are for one of the Pt atoms labeled "1" in Figure 10. [b] The values listed are for one of the Sn atoms labeled "2" in Figure 10. [c] From ref 20. All of the Pt atoms are equivalent in this cluster.

type and size provide the basic bonding interactions that occur in bimetallic systems.[20,33,43] In Table 1 are listed calculated values[44] for the charges and orbital populations of Pt atoms in the Pt_{15} and Sn_4Pt_{11} clusters. For comparison we also include results obtained[20] for two "cubic" clusters, Pt_8 and Pt_4Sn_4. In the Pt_4Sn_4 cluster, the Pt and Sn atoms alternate in the corners of a cube in such a way that each Pt atom has three Sn nearest neighbors (see cluster II in ref 33b). After examining the electronic properties of a series of Pt−Sn clusters at the ab initio SCF level,[20] we found a small shift of 5s,p electrons from Sn toward Pt. This is consistent with the fact that Pt has a bigger Pauling electronegativity than Sn.[45,46] Several authors have postulated a Sn → Pt charge transfer in Sn/Pt alloys to explain their experimental data.[13,47] The formation of Pt−Sn bonds leads to an increase in the Pt 6s,p electron population and a decrease in the Pt 5d population (phenomena equivalent to a d → s,p rehybridization that moves electrons from around Pt into the Pt−Sn bond).[20] Measurements of the Pt L_{II}-edge in XANES (X-ray absorption near-edge spectroscopy) show that the Pt atoms in PtSn and $PtSn_2$ alloys have a 5d electron population smaller than that of the Pt atoms in metallic Pt.[46] The reduction in the Pt 5d population can explain why the density of states near the Fermi edge in a bulk Pt_3Sn alloy is much smaller than that in metallic Pt.[13] It is well-known that Pt acts as a (6s,p)-electron acceptor and a (5d)-electron donor when making intermetallic and inorganic compounds.[33,46,48] In Sn/Pt alloys, both metals accumulate electrons around the Pt−Sn bonds.[20] This type of bonding has been seen in several bimetallic systems that contain Pt[33] or other group 10 metals,[9] and it can lead to a significant decrease in the chemical activity of the bonded metals.[8]

SO_2 has a large electron affinity (∼1.1 eV)[49] and behaves as an electron acceptor when bonded to metals.[38,50−52] The transfer of electrons from the metal into the LUMO of SO_2 ($3b_1$ orbital) plays a predominant role in the energetics of metal−SO_2 bonds.[53] The results in Table 1 indicate that the tin atoms in a Sn/Pt alloy should be less reactive toward SO_2 than the atoms in pure metallic tin. Once Sn "loses" valence 5s and 5p electrons, this metal cannot respond in an effective way to the presence of SO_2. In the case of the Pt atoms in the alloy, a prediction of their behavior is not straightforward because these atoms "gain" 6s and 6p electrons but "lose" 5d electrons. To determine which of these processes is more important, we examined the adsorption of SO_2 on a-top and bridge Pt sites of clusters I and II using ab initio SCF calculations.

Figure 10 shows the bonding configurations of SO_2. Previous experimental and theoretical works indicate that the molecule adsorbs with these orientations on metal surfaces.[5,27a,38,51] On Pt(111), two adsorption states have been observed for SO_2.[26] In one of them, the results of HREELS[5] and NEXAFS[27a] indicate that SO_2 is adsorbed with its molecular plane essentially perpendicular to the surface, probably in a η^2-S,O bonding configuration.[5] Table 2 lists the structural parameters and bonding energies derived at the ab initio SCF level for the adsorption of SO_2 on clusters I and II. The predicted SO_2 geometries and Pt−S (2.32−2.40 Å) and Pt−O (2.12−2.17 Å) bond lengths are close to those observed in inorganic complexes.[54] It is likely that the values listed in the table

(43) (a) Castellani, N. J.; Legare, P. *J. Phys. Chem.* **1994**, *98*, 9606. (b) Rochefort, A.; Fournier, R. *J. Phys. Chem.* **1996**, *100*, 13506. (c) Ferullo, R. M.; Castellani, N. *Langmuir* **1996**, *12*, 70. (d) Illas, F.; López, N.; Ricart, J. M.; Clotet, A.; Conesa, J. C.; Fernández-García, M. *J. Phys. Chem. B* **1988**, *102*, 141−147.

(44) (a) The charges and orbital populations were calculated by a Mulliken population analysis.[44b] Due to the limitations of this type of analysis,[44c] the reported values must be considered only in qualitative terms. (b) Mulliken, R. S. *J. Chem. Phys.* **1955**, *23*, 1841. (c) Szabo, A.; Ostlund, N. S. *Modern Quantum Chemistry*; McGraw-Hill: New York, 1989.

(45) Allred, A. L. *J. Inorg. Nucl. Chem.* **1961**, *17*, 215.

(46) Jeon, Y.; Chen, J.; Croft, M. *Phys. Rev. B* **1994**, *50*, 6555.

(47) Stagg, S. M.; Querini, C. A.; Alvarez, W. E.; Resasco, D. E. *J. Catal.* **1997**, *168*, 75 and references therein.

(48) (a) Apai, G.; Baetzold, R. C.; Jupiter, P. J.; Viescas, A. J.; Lindau, I. *Surf. Sci.* **1983**, *134*, 122. (b) Horsley, J. A. *J. Chem. Phys.* **1982**, *76*, 1451. (c) Hay, P. J. *J. Am. Chem. Soc.* **1981**, *103*, 1390.

(49) Nimlos, M. R.; Ellison, G. B. *J. Phys. Chem.* **1986**, *90*, 2574.

(50) Rodriguez, J. A. *Surf. Sci.* **1990**, *226*, 101.

(51) Sellers, H.; Shustorovich, E. *Surf. Sci.* **1996**, *346*, 322.

(52) Mingos, D. M. P *Transition Met. Chem.* **1978**, *3*, 1.

(53) (a) Sakaki, S.; Sato, H.; Imai, Y.; Morokuma, K.; Ohkubo, K. *Inorg. Chem.* **1985**, *24*, 4538. (b) Pacchioni, G.; Clotet, A.; Ricart, J. M. *Surf. Sci.* **1994**, *315*, 337.

(54) Wilkinson, G., Gillard, R. D., McCleverty, J. A., Eds. *Comprehensive Coordination Chemistry*; Pergamon Press: New York, 1987; Chapters 16 and 52.

Table 2. Adsorption of SO_2 on Pt and Pt−Sn Clusters

	geometry				adsorption energy (kcal/mol)[a]
	Pt_1−S(Å)	Pt_1−O(Å)	S−O(Å)	O−S−O(deg)	
free SO_2			1.42	118	
on Pt(111), Pt_{15}					
η^1-S a-top	2.34		1.43	118	6
η^1-S bridge	2.37		1.46	119	9
η^2-O,O bridge		2.12	1.50	123	14
η^2-O,S bridge	2.38	2.16	1.51	120	13
			(1.45)[b]		
on Sn/Pt(111), $Pt_{11}Sn_4$					
η^1-S a-top	2.36		1.42	118	3
η^1-S bridge	2.38		1.46	119	7
η^2-O,O bridge		2.13	1.48	121	11
η^2-O,S bridge	2.40	2.17	1.49	121	12
			(1.44)[b]		

[a] Positive values denote an exothermic process. [b] Oxygen atom nonbonded to platinum.

underestimate the adsorption energy of SO_2 on Pt(111) and $(\sqrt{3} \times \sqrt{3})$R30°-Sn/Pt(111) due to the lack of electron correlation in our calculations.[34] When dealing with adsorption energies, we will focus our attention on qualitative trends (see Section II.2). For the bonding configurations in Figure 10, the strength of the Pt−SO_2 adsorption bond increases in the following sequence: η^1-S a-top < η^1-S bridge < η^2-S,O bridge ≈ η^2-O,O bridge. The calculated adsorption energies for the η^2-S,O and η^2-O,O coordinations are very close, and the SCF results really cannot be used to predict which of these configurations is more stable. Nevertheless, they are clearly more stable than the η^1-S configurations, and the two adsorption states observed in photoemission experiments for SO_2 on Pt(111) probably correspond to η^2-S,O and η^2-O,O bonded SO_2.

A comparison of the adsorption energies of SO_2 on the Pt_{15} and $Pt_{11}Sn_4$ clusters shows that on Pt sites of the bimetallic system the bonding interactions with the molecule are weaker (3−1 kcal/mol) than on similar sites of the pure Pt cluster. The Pt(5d) → Pt(6s,6p) rehybridization induced by alloying concentrates electrons in the regions around the Pt−Sn bonds making more difficult the Pt ↔ SO_2 bonding interactions. On the Pt_{15} cluster, the SCF calculations showed net electron transfers[44] from the metal into the LUMO of SO_2, a behavior consistent with results of UPS studies which indicate that this orbital is populated when SO_2 chemisorbs on Pt(111).[5] For adsorption of SO_2 on the $Pt_{11}Sn_4$ cluster, the electron density[44] on the molecule was 0.1−0.2e smaller than on the Pt_{15} cluster. Valence photoemission spectra show that the density of states near the Fermi edge in tin platinum alloys is much smaller than in pure metallic platinum.[13] This together with the drop in the Pt 5d population induced by bimetallic bonding (Table 1 and refs 20 and 46) make platinum less reactive toward electron-acceptor species such as SO_2 (Table 2), S,[20] C_2H_4,[15] CO,[13,16,15] and NO.[14] In the case of SO_2 on Pt(111), the increase in the electron population of the adsorbate's LUMO (S−O antibonding) leads to an elongation of the S−O bonds facilitating the dissociation of the molecule. On $Pt_{11}Sn_4$, the electron population of the SO_2 LUMO is lower than on Pt_{15}, and therefore, the perturbations in the structural geometry of the adsorbate are smaller on the bimetallic system.

The results in Tables 1 and 2 indicate that the experimental trends seen in Figure 9 reflect changes that take place in the electronic properties of the metals (electronic effects). It is well-established nowadays that metal−metal bonding (or alloying) can induce substantial modifications in the chemical and catalytic properties of metals,[8−11,17] but very few systems show changes in reactivity as drastic as those seen for the SO_2/Sn/Pt(111) system.[8] The large chemical affinity that Sn has for SO_2 practically disappears upon alloying of this metal, and the chemical activity of Pt also drops. The Sn/Pt system illustrates how a redistribution of electrons that occurs in bimetallic bonding can be useful for the design of catalysts that are less sensitive to the presence of SO_2 and other sulfur-containing molecules in the feedstream.

Cu, Ag, and Sn are added to Pt catalysts to improve their selectivity for the reforming of hydrocarbons.[1,55] In this respect the effects of the admetals are more or less similar. The basic idea is to use Cu, Ag, and Sn as site blockers to "remove" the large ensembles of Pt atoms that carry out C−C hydrogenolysis and leave small Pt ensembles on which the isomerization of hydrocarbons can take place.[2c,11] Previously, we have found that Cu and Ag promote Pt ↔ S interactions and the formation of platinum sulfides.[18,19] Tin does not have this "ability". After Cu, Zn, or Al on Pt(111) are deposited, one sees the formation of alloys.[19,56] These alloys break apart in the presence of sulfur-containing molecules.[19,56] In the Sn/Pt system, the stability of the alloys is high, and there are substantial changes in the electronic properties of the metals. The combination of these factors produces a bimetallic system that has a remarkably low reactivity toward sulfur-containing molecules. When compared to other admetals (Cu,[19] Ag,[18] Au,[18b] Zn,[19] Al),[56] tin is the best choice when selecting a site blocker and trying to minimize the sensitivity of Pt-reforming catalysts toward sulfur poisoning.

IV. Summary and Conclusions

Metallic tin has a large chemical affinity for SO_2. At 100−150 K, SO_2 disproportionates on polycrystalline tin forming multilayers of SO_3 ($2SO_{2,a} \rightarrow SO_{gas} + SO_{3,a}$). At these low temperatures, the full dissociation of adsorbed SO_2 ($SO_{2,a} \rightarrow S_a + 2O_a$) is minimal. As the temperature is raised to 300 K, the SO_3 decomposes yielding SO_4, S, and O on the surface. These species are also produced when SO_2 is dosed to polycrystalline tin at 300 K. At room temperature, there is extensive dissociation of SO_2 on the tin surface, and the adsorbed SO_3 and SO_4 species are probably formed by the reaction of SO_2 with adsorbed O. Pure tin exhibits a much higher reactivity toward SO_2 than late transition metals (Ni, Pd, Pt, Cu, Ag, Au).

(55) (a) Ponec, V. *Adv. Catal.* **1983**, *32*, 149. (b) Clarke, J. K. A. *Chem. Rev.* **1975**, *75*, 291.
(56) Rodriguez, J. A.; Kuhn, M. *J. Vac. Sci. Technol. A* **1997**, *15*, 1608.

In contrast, tin atoms in contact with Pt(111) interact weakly with SO_2. A $(\sqrt{3} \times \sqrt{3})$R30°-Sn/Pt(111) alloy is less reactive toward SO_2 than polycrystalline tin or clean Pt(111). On the alloy, no SO_3 or SO_4 species are formed at temperatures between 100 and 300 K. At 100 K, SO_2 adsorbs molecularly on $(\sqrt{3} \times \sqrt{3})$R30°-Sn/Pt(111). Most of the adsorbed SO_2 desorbs intact from the surface (250−300 K), whereas a small fraction dissociates into S and O. The drop in reactivity when going from pure tin to the $(\sqrt{3} \times \sqrt{3})$R30°-Sn/Pt(111) alloy can be attributed to a combination of ensemble (lack of adsorption sites with two or three adjacent tin atoms in the alloy) and electronic effects (reduction in the valence 5s,p electron population of tin induced by bimetallic bonding). On the other hand, the low reactivity of the Pt sites in $(\sqrt{3} \times \sqrt{3})$R30°-Sn/Pt(111) with respect to Pt(111) is a consequence of electronic effects; alloying decreases the density-of-states of the Pt 5d band near the Fermi level, and a Pt(5d) → Pt(6s,6p) rehybridization localizes electrons in the regions around the Pt−Sn bonds, reducing the electron-donor ability of the Pt atoms. The Sn/Pt system illustrates how a redistribution of electrons that occurs in bimetallic bonding can be useful for the design of catalysts that are less sensitive to the presence of SO_2 and other sulfur-containing molecules.

Acknowledgment. This work was carried out at Brookhaven National Laboratory and supported by the U.S. Department of Energy (Contract No. DE-AC02-98CH10886), Office of Basic Energy Sciences, Chemical Science Division. The NSLS is supported by the divisions of Materials and Chemical Sciences of the U.S. Department of Energy. T.J. acknowledges the support of a NATO grant awarded in 1997.

JA982174A